

# ADVERSARIAL OBJECT HALLUCINATION ATTACKS IN VIDEO-LANGUAGE MODELS VIA INTERMEDIATE FEATURE ALIGNMENT

006 **Anonymous authors**

007 Paper under double-blind review

## ABSTRACT

013 Video Large Language Models (Vid-LLMs) have rapidly advanced video under-  
014 standing, yet their robustness against semantic adversarial manipulation, espe-  
015 cially object hallucination, remains largely unexplored. We introduce Adversarial  
016 Object Hallucination (AOH), a novel attack that compels Vid-LLMs to “see” non-  
017 existent objects in videos by injecting visually imperceptible perturbations. Un-  
018 like prior attacks limited to inputs or outputs of videos, AOH directly manipulates  
019 intermediate connector features, aligning them with representations from a target  
020 video to induce controllable hallucinations. To systematically assess this threat,  
021 we curate a benchmark of 535 clean/target video pairs with high-quality VQA  
022 annotations. Extensive experiments show that AOH poses a severe threat to state-  
023 of-the-art Vid-LLMs, achieving highly effective attacks with alarming *cross-scale*  
024 *transferability*: adversarial examples optimized on smaller models transfer even  
025 more strongly to larger counterparts of the same architecture, amplifying attack  
026 impact while reducing adversarial cost. Further analyses reveal that perturbations  
027 encode semantic object contours, while Grad-CAM highlights their covert influ-  
028 ence. These findings expose a severe and previously overlooked vulnerability in  
029 Vid-LLMs, raising urgent concerns about their secure deployment and providing  
030 a foundation for future adversarial research in video-language modeling.

## 1 INTRODUCTION

031 In recent years, with the rapid advancements in deep learning, multimodal large models, especially  
032 Video Large Language Models (Vid-LLMs), have demonstrated unprecedented capabilities in un-  
033 derstanding and reasoning about video content. By integrating powerful vision encoders with large  
034 language models, these models can perform semantic analysis of complex video events, answer  
035 open-ended questions, and generate detailed descriptions, showcasing immense potential in critical  
036 domains such as autonomous driving, intelligent surveillance, and content creation. Prominent ex-  
037 amples include models like Video-ChatGPT (Maaz et al., 2024), VideoLLaMA (Zhang et al., 2023;  
038 Cheng et al., 2024; Zhang et al., 2025a), and InternVL (Chen et al., 2023).

039 However, the powerful capabilities of these models are accompanied by growing concerns regard-  
040 ing their security and robustness. In the image domain, adversarial attacks have become a mature  
041 research area, where attackers can induce models to make erroneous classifications, detections, or  
042 interpretations by adding subtle, often imperceptible, perturbations to images (Zhao et al., 2023;  
043 Hu et al., 2025; Wang et al., 2024; Zhang et al., 2025b). Despite this, the adversarial robustness  
044 of Vid-LLMs, particularly against semantic adversarial attacks that induce models to “see” specific,  
045 non-existent objects (i.e., object hallucination), remains a largely unexplored frontier in the dynamic  
046 and high-dimensional video domain. The temporal coherence and high dimensionality of video data  
047 pose unique challenges for generating adversarial examples, making existing image attack methods  
048 difficult to directly extend. This under-explored vulnerability, if exploited maliciously, could lead to  
049 severe consequences in critical applications MacLeod et al. (2017), such as misidentifying obstacles  
050 in autonomous driving systems or generating false alarms in security surveillance.

051 To bridge this critical gap, we propose Adversarial Object Hallucination (AOH), a novel adversarial  
052 attack. AOH aims to mislead Vid-LLMs into erroneously perceiving and reporting specific, non-

existent target objects within a video by introducing visually subtle perturbations to clean videos. Unlike prior attacks that directly manipulate the model’s final output, our method uniquely focuses on manipulating the intermediate “Connector” feature representations within Vid-LLMs. We achieve this by aligning the intermediate features of an adversarial video with features derived from a pre-defined target video containing the desired object, thereby implanting the target object’s semantic information deep within the model’s internal representations.

To address the challenge of a lack of dedicated benchmark datasets for such attack tasks, we meticulously curate a comprehensive multi-source dataset. This dataset comprises 535 pairs of clean/target videos, rigorously annotated with Visual Question Answering (VQA) pairs, providing a robust foundation for comprehensively evaluating the vulnerability of Vid-LLMs to adversarial object hallucination attacks.

Concentrating on adversarial visual inputs, our work is distinct from previous adversarial attacks in two key aspects:

- **Attack Objective:** Our AOH attack aims to induce the *fabrication of non-existent semantic content* (i.e., object hallucination) within Vid-LLMs’ understanding, leading to erroneous perceptions of objects that are not truly present. This fundamentally differs from traditional adversarial objectives like misclassification of existing objects, triggering harmful text outputs, or bypassing safety alignments. We focus on injecting a specific, fabricated visual semantic concept.
- **Attack Mechanism and Efficiency:** We achieve this through a intermediate feature alignment strategy, directly manipulating the high-level multimodal representations within the Vid-LLM’s “Connector”. Crucially, our findings reveal an alarming *cross-scale transferability*: adversarial examples generated for smaller models not only transfer successfully but often achieve *superior attack performance* on larger, more complex Vid-LLMs of the same architecture. This implies a potentially more efficient and lower-cost attack paradigm, as adversaries could target smaller, more accessible models to compromise larger, deployed systems.

In summary, our work not only uncovers a severe and insidious vulnerability in the semantic adversarial robustness of Vid-LLMs but also provides a pioneering framework for evaluating and understanding this vulnerability. Our findings emphasize the urgent need for developing Vid-LLMs with more robust internal representations and lay a foundational framework for future research in adversarial machine learning and multimodal AI safety. Our main contributions are as follows:

- We systematically investigate adversarial object hallucination in Vid-LLMs, revealing these models’ susceptibility to semantic adversarial attacks in the video domain.
- We propose AOH, a novel attack method, which manipulates the intermediate “Connector” feature representations of Vid-LLMs to generate visually subtle adversarial video perturbations that efficiently induce precise object hallucinations.
- We construct and release the comprehensive benchmark dataset for video object hallucination attacks. This dataset includes 535 high-quality clean/target video pairs with rigorous VQA annotations, and due to its unique construction, it also holds potential value for related video editing tasks such as object removal.
- We conduct in-depth analyses of AOH’s stealthiness. Using explainability tools like GradCAM, we confirm that the models’ attention remains focused on naturally occurring regions in the video, rather than aberrantly on the hallucinated regions, when subjected to AOH attacks.

## 2 RELATED WORK

### 2.1 VIDEO LARGE LANGUAGE MODELS

The rapid advancements in Large Language Models (LLMs) such as GPT (Brown et al., 2020) and LLaMA (Touvron et al., 2023) have revolutionized natural language processing. This success has naturally extended to multimodal domains, leading to the development of Vision-Language Models (VLMs) that integrate visual information with text, exemplified by LLaVA (Liu et al., 2023) and MiniGPT-4 (Zhu et al., 2024). Building upon VLMs, Video LLMs (Vid-LLMs) further incorporate temporal dynamics to understand and reason about video content. These models typically consist

108 of a visual encoder (e.g., based on ViT or CLIP), a connector module to project visual features into  
 109 the language model’s embedding space, and a large language model (LLM) for conversational un-  
 110 derstanding and response generation. Prominent Vid-LLMs include Video-ChatGPT (Maaz et al.,  
 111 2024), VideoLLaMA (Zhang et al., 2023; Cheng et al., 2024; Zhang et al., 2025a), InternVL (Chen  
 112 et al., 2023), and LLaVA-OneVison (Li et al., 2025). These models excel in tasks such as video  
 113 question answering (VQA) and video captioning, demonstrating sophisticated spatio-temporal rea-  
 114 soning capabilities. Current research primarily focuses on enhancing their performance, efficiency,  
 115 and generalization across diverse video tasks.

## 116 2.2 ADVERSARIAL ROBUSTNESS OF LARGE MODELS

118 Adversarial attacks aim to mislead machine learning models by introducing subtle, often impercep-  
 119 tible, perturbations to their inputs. This field originated with attacks against image classifica-  
 120 tion models, demonstrating vulnerabilities through techniques like FGSM (Goodfellow et al., 2015) and  
 121 PGD (Madry et al., 2018). Extensive research has since focused on both developing novel attacks  
 122 and designing robust defenses in computer vision.

123 The concept of adversarial robustness has also been extended to other modalities. In Language Mod-  
 124 els (LLMs), attacks typically involve textual perturbations such as typos, paraphrasing, or prompt  
 125 engineering to induce factual errors, sentiment shifts, or jailbreaking behaviors (Zou et al., 2023; Yi  
 126 et al., 2024; Jin et al., 2024). The focus here is often on semantic shifts and maintaining fluency  
 127 while causing misinterpretation.

128 With the rise of multimodal models, robustness research has naturally expanded. Initial efforts  
 129 investigated adversarial attacks against Vision-Language Models (VLMs), primarily in image-text  
 130 scenarios (Zhou et al., 2024). These attacks aim to deceive VLMs in tasks like image captioning or  
 131 visual question answering by perturbing images or text inputs, or both simultaneously. For instance,  
 132 some work explores targeted attacks to make VLMs return predefined responses or misinterpret  
 133 image content (Zhao et al., 2023; Hu et al., 2025; Wang et al., 2024; Zhang et al., 2025b). While  
 134 these studies highlight vulnerabilities in multimodal understanding, they predominantly focus on  
 135 static image-text inputs or broader unimodal attacks. Critically, although recent works have begun to  
 136 address specific attacks on video-based models (Li et al., 2024; Huang et al., 2025), the adversarial  
 137 robustness of Vid-LLMs, particularly concerning semantic manipulations such as inducing object  
 138 hallucination within video sequences, remains a nascent and significantly under-explored area. Our  
 139 work fills this gap by specifically targeting Vid-LLMs with semantic object hallucination attacks.

## 140 3 DATASET CONSTRUCTION

141 The task of adversarial object hallucination in Vid-LLMs necessitates a specialized dataset comprising  
 142 clean video, target video, and corresponding ground-truth information such as object masks and  
 143 VQA pairs. However, such a comprehensive benchmark is currently unavailable. To address this  
 144 critical data scarcity and enable robust evaluation, we meticulously curate a multi-source benchmark  
 145 dataset. This section details our data collection strategies, human annotation processes, and VQA  
 146 generation methodology.

147 Our ideal approach to construct video pairs involves professionally adding realistic entities into clean  
 148 videos to obtain (clean video, target video, target mask) triplets. While this offers high fidelity, it  
 149 is technically demanding and highly time-consuming. To maximize data acquisition efficiently, we  
 150 adopt a multi-pronged strategy: (1) leveraging existing public datasets that contain original and ma-  
 151 nipulated videos; (2) judiciously employing professional video editing for specific scenarios; and (3)  
 152 ingeniously utilizing a “reverse thinking” approach by treating videos with existing objects as “target  
 153 videos” and applying object removal techniques to generate corresponding “clean videos.” This last  
 154 strategy significantly expands our data pool, provided the removal quality is visually convincing.

### 155 3.1 DATA SOURCES

156 We integrate and refine videos from four distinct sources to build our comprehensive dataset:

- 157 • **HQVI Dataset (Cho et al., 2025):** This dataset provides high-quality, realistic Video Inpainting  
 158 (VI) benchmark videos, synthesized by compositing objects from VideoMatte240K (Lin et al.,

162 2021) onto real-world Pexels videos using fine alpha mattes. HQVI offers multiple resolutions;  
 163 considering that most video models compress resolution, we selected the 480P version, which  
 164 suffices for most experimental model requirements. This dataset supplies 10 videos.

165 • **ROVI Dataset (Wu et al., 2024):** ROVI is a pioneering dataset for object removal, containing  
 166 triplets of original videos, removal expressions, and inpainted videos. For our “reverse think-  
 167 ing” approach, we treat the original videos as “target videos” and the inpainted videos as “clean  
 168 videos.” To ensure the highest visual realism for our “clean” videos (i.e., successfully removed ob-  
 169 jects), we introduced a rigorous human evaluation process. Three human annotators independently  
 170 scored each inpainted video on a 5-point scale (with 5 being the best) across four dimensions: 1)  
 171 Spatial Coherence / Visual Realism, 2) Temporal Consistency, 3) Artifact Severity, and 4) Overall  
 172 Removal Quality. We aggregated scores from the three annotators and filtered for high-quality  
 173 videos with a total score of 14 or 15. Due to challenges in providing adequate entity descrip-  
 174 tions or persistent unnatural artifacts in some videos, we ultimately selected 468 videos for further  
 175 annotation from the original 2,967 A2D-Sentences videos and 2,683 Refer-YouTube-VOS videos.

176 • **Video-Sham Dataset (Mittal et al., 2023):** VideoSham is a video manipulation dataset featuring  
 177 diverse, context-rich, human-centric manipulated videos created by professional video editors. We  
 178 specifically selected videos from the “Adding an entity” and “Removing an entity” tasks. From  
 179 “Adding an entity”, we obtained 45 videos where the manipulated version serves as the “target  
 180 video” and the original as the “clean video”. For the “Removing an entity” task, similar to ROVI,  
 181 we applied the same rigorous human filtering process to ensure high quality for the “clean videos”,  
 182 yielding 22 videos. In total, 67 videos were sourced from Video-Sham.

183 • **Custom Driving Dataset:** Recognizing the scarcity of driving scenarios in existing datasets—a  
 184 crucial domain due to its implications for autonomous driving safety—we curated a bespoke  
 185 dataset. This was constructed using real objects (e.g., vehicles, pedestrians, road signs) from  
 186 the BDD100K dataset (Yu et al., 2020) within realistic driving scenes, employing alpha composi-  
 187 tion via DaVinci Resolve video editing software, a process akin to HQVI. This dataset explicitly  
 188 includes target masks. We generated 10 videos for this specific context.

189 In total, our benchmark dataset comprises **535 clean/target video pairs**, providing a robust founda-  
 190 tion for evaluating adversarial object hallucination.

### 192 3.2 VQA ANNOTATION

194 Accurate and unambiguous Visual Question Answering (VQA) pairs are essential for evaluating  
 195 object hallucination attacks. We designed a multi-stage annotation pipeline leveraging both large  
 196 language models (LLMs) and human expertise:

1. **Initial Information Acquisition:** For all target videos, we first gather essential auxiliary infor-  
 198 mation: video descriptions (pre-generated by VideoLLaMA3-7B and refined by human annota-  
 199 tors), target entity masks (obtained using Segment Anything 2 (Ravi et al., 2025)), and target  
 200 entity text descriptions (manually added). For the ROVI dataset, which inherently provides these  
 201 data, we directly utilized its existing annotations.
2. **VQA Pre-generation:** Leveraging advanced LLMs, specifically GPT-4o, Claude-3.5-Sonnet,  
 203 and DeepSeek-V3, we pre-generate VQA pairs. This process utilizes the target video’s descrip-  
 204 tion and the target entity’s information to formulate pertinent questions regarding the presence  
 205 and characteristics of the target object.
3. **VQA Refinement and Validation:** To minimize potential linguistic ambiguity or factual errors  
 207 in the pre-generated VQA, we employ an iterative refinement process. The VQA pairs are tested  
 208 against sampled frames (e.g., 4 frames) from the target video using the web-based ChatGPT.  
 209 Based on the model’s feedback and human review, the VQA pairs are repeatedly optimized until  
 210 they are clear, precise, and accurately reflect the presence or absence of the target object.

## 212 4 ATTACK METHOD

214 This section formally introduces Adversarial Object Hallucination (AOH), our proposed white-box  
 215 attack against Video Large Language Models. We begin by defining the threat model and then detail

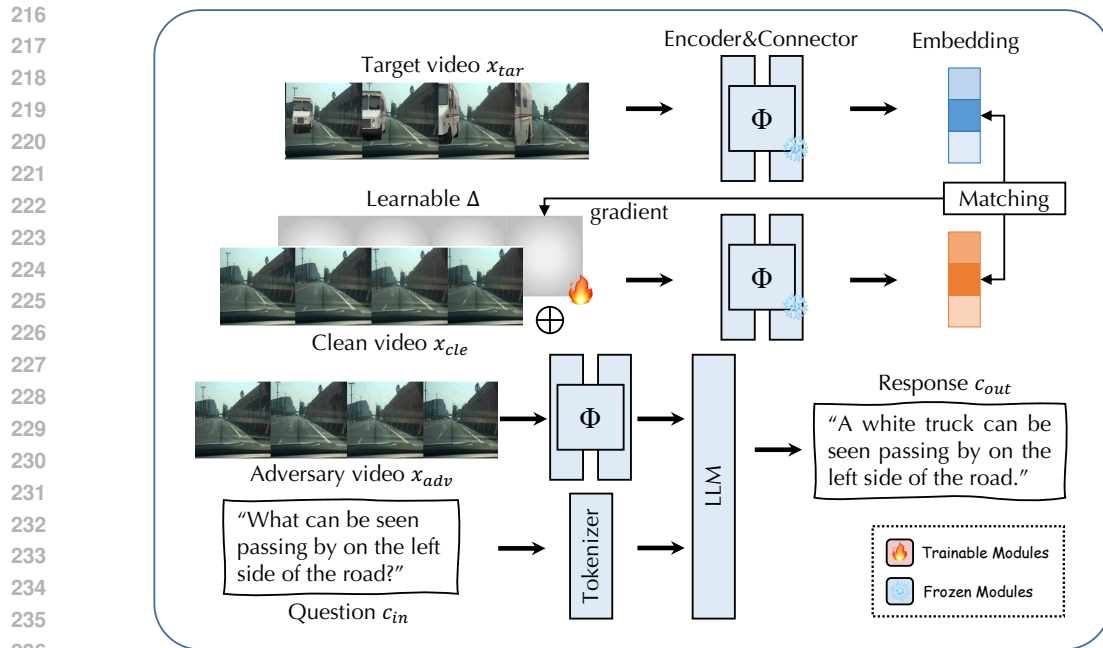


Figure 1: Pipelines of our attacking strategies.

our objective function, which leverages intermediate feature alignment to induce object hallucination with visually subtle perturbations.

#### 4.1 THREAT MODEL

We denote a Vid-LLM as  $F(x_v; c_{in}) \mapsto c_{out}$ , where  $x_v$  is the input video,  $c_{in}$  is the input text (e.g., a question), and  $c_{out}$  is the generated output text (e.g., an answer). The typical architecture of a Vid-LLM comprises a Vision Encoder and a Connector module, which together project the raw video input into the language model’s embedding space. For simplicity, we denote this combined intermediate feature extraction process as  $\Phi(x_v)$ , where  $\Phi(x_v)$  represents the output feature tensor from the Connector module for video  $x_v$ . Thus, the internal processing can be abstracted as  $L(\Phi(x_v); c_{in}) \mapsto c_{out}$ .

Our threat model specifies the adversarial conditions (Carlini et al., 2019) adapted for generating object hallucinations in Vid-LLMs:

- 1. Adversary Knowledge:** The adversary is assumed to have *white-box access* to the victim Vid-LLM,  $F$ . This includes full knowledge of its architecture and weights, particularly those of the Vision Encoder and the Connector module (i.e., access to  $\Phi(\cdot)$ ).
- 2. Adversary Goals:** The adversary’s primary goal is *targeted object hallucination*. Specifically, given a clean video  $x_{cle}$  and a target object, the adversary aims to generate an adversarial video  $x_{adv}$  such that the Vid-LLM  $F$  perceives the target object as present in  $x_{adv}$ , even though it is absent in  $x_{cle}$ . This perception is evidenced by the model’s VQA responses on meticulously designed benchmark.
- 3. Adversary Capabilities:** The adversary can manipulate the input video  $x_v$  to generate  $x_{adv}$  by adding perturbations. The most critical constraint is imposed by the  $\ell_p$  budget, ensuring the perturbations are *visually subtle*. We adopt the commonly used  $\ell_\infty$  norm, such that  $\|x_{cle} - x_{adv}\|_\infty \leq \epsilon$ , where pixel values are in  $[0, 255]$ . Additionally, the adversary is *forbidden to manipulate the input text  $c_{in}$* .

**Remark.** Our work investigates a challenging and realistic white-box threat model where the adversary leverages detailed model knowledge to induce specific semantic hallucinations with subtle perturbations in the high-dimensional video domain. Critically, while our attack is designed under white-box assumptions, our subsequent experiments reveal a remarkable **cross-scale transferability**

270 of these adversarial examples, indicating a broader and more concerning vulnerability in Vid-LLMs  
 271 beyond the direct white-box setting.  
 272

#### 273 4.2 INTERMEDIATE FEATURE ALIGNMENT 274

275 Figure 1 show the pipeline of our attacking strategies. Our AOH attack is designed to implant  
 276 the semantic presence of a target object by aligning the intermediate feature representations of the  
 277 adversarial video with those derived from a target video containing the desired object. Given a clean  
 278 video  $x_{cle}$  and a target video  $x_{tar}$  (which contains the object we wish to hallucinate in  $x_{cle}$ ), our  
 279 objective is to find an adversarial video  $x_{adv}$  such that:

$$280 \quad x_{adv} = \arg \max_{\|x_{cle} - x_{adv}\|_{\infty} \leq \epsilon} \cos\_sim(\Phi(x_{adv}), \Phi(x_{tar})) \quad (1)$$

282 Here,  $\cos\_sim(\cdot, \cdot)$  represents the cosine similarity between the intermediate feature tensors from  
 283 the  $\Phi$  module for the adversarial video and the target video. By maximizing this similarity, we  
 284 encourage the Vid-LLM’s internal representation for  $x_{adv}$  to embed the semantic information of the  
 285 object present in  $x_{tar}$ , without directly manipulating the final text output layer. This approach subtly  
 286 guides the model’s perception at an earlier, feature-level stage, making the attack more robust and  
 287 covert.

288 The constrained optimization problem in Equation (1) is solved iteratively using Projected Gradient  
 289 Descent (PGD) (Madry et al., 2018). Specifically, for each iteration  $t$ :

$$290 \quad x_{adv}^{(t+1)} = \text{Clip}_{x_{cle}, \epsilon} \left[ x_{adv}^{(t)} + \alpha \cdot \text{sign} \left( \nabla_{x_{adv}^{(t)}} \cos\_sim(\Phi(x_{adv}^{(t)}), \Phi(x_{tar})) \right) \right] \quad (2)$$

292 where  $\alpha$  is the step size, and  $\text{Clip}_{x_{cle}, \epsilon}(\cdot)$  projects the perturbed video back into the  $\epsilon$ -neighborhood  
 293 of the clean video  $x_{cle}$  after each step, ensuring the  $\ell_{\infty}$  perturbation budget is maintained. This  
 294 iterative process allows us to subtly inject the target object’s semantics into the video’s intermediate  
 295 representations, leading to the desired object hallucination by the Vid-LLM.

## 296 5 EXPERIMENTS

### 297 5.1 EXPERIMENTAL SETUP

300 All experiments were conducted on computing resources equipped with a NVIDIA 4090 GPU. Our  
 301 experimental pipeline involves generating adversarial video samples using AOH, then evaluating  
 302 the target Vid-LLMs’ responses to both clean and adversarial videos using a meticulously designed  
 303 VQA-based assessment framework.

305 **Target Video-Language Models** To provide a broad assessment of Vid-LLM vulnerabilities, we  
 306 evaluate AOH against a diverse set of prominent open-source Vid-LLMs, selected for their varying  
 307 architectures and scales. For consistency and resource efficiency, we used their default parameter  
 308 settings but uniformly adjusted the sampled frame rate to 8 frames per video. Additionally, in line  
 309 with prior work (Zhang et al., 2023; Cheng et al., 2024; Zhang et al., 2025a), the temperature setting  
 310 for response generation is set to 0 during evaluation to ensure deterministic outputs:

- 311 • **Video-ChatGPT (Maaz et al., 2024)**: A 7B parameter model known for its strong video under-  
 312 standing capabilities.
- 313 • **VideoLLaMA3 (Zhang et al., 2025a)**: We experimented with both the 2B and 7B parameter ver-  
 314 sions of this model. A crucial consideration for VideoLLaMA3 is its dynamic resolution handling,  
 315 which can lead to significant memory consumption for high-resolution videos<sup>1</sup>. To balance model  
 316 accuracy and memory usage, we adaptively scaled its input resolution, restricting it to not exceed  
 317 480P (854x480) while maintaining aspect ratio. This adjustment ensures its maximum input size  
 318 still generally exceeds that of other models in our experiments.
- 319 • **InternVL 2.5 (Chen et al., 2023)**: This model family offers a range of scales, and we tested the  
 320 1B, 2B, 4B, and 8B parameter variants.
- 321 • **LLaVA-OneVison (Li et al., 2025)**: We evaluated the 0.5B and 7B parameter versions of LLaVA-  
 322 OneVison, which serve as key models for analyzing cross-scale transferability.

323 <sup>1</sup><https://github.com/DAMO-NLP-SG/VideoLLaMA3/issues/82>

324     **Evaluation Metrics** Following established practices in evaluating VQA performance for multi-  
 325     modal models (Maaz et al., 2024), we employ two primary metrics to quantify the success of object  
 326     hallucination attacks and the overall video understanding capabilities of Vid-LLMs:  
 327

- 328     • **Accuracy:** This metric measures the binary correctness of a model’s “yes/no” answer to a ques-  
 329     tion. For clean videos, a high Acc indicates accurate understanding of the absence of the target  
 330     object. For adversarial videos, a low Acc (i.e., incorrect “no” answer) or a high Acc (i.e., incorrect  
 331     “yes” answer that aligns with hallucination) indicates successful deception.
- 332     • **ChatGPT-3.5 Assisted Scoring (0-5 Scale):** Inspired by previous work (Maaz et al., 2024), we  
 333     utilize GPT-3.5 to provide a more nuanced qualitative assessment of the model’s generated re-  
 334     sponses. For each VQA pair, GPT-3.5 evaluates the model’s answer against the ground-truth  
 335     answer (for clean videos) or the target answer (for adversarial videos), assigning a score from 0  
 336     (completely incorrect/irrelevant) to 5 (excellent, semantically aligned, and detailed). High scores  
 337     on clean videos reflect strong baseline understanding. For adversarial videos, high scores indicate  
 338     that the model not only perceived the hallucinated object but also provided semantically rich and  
 339     accurate details about it, signifying a more profound attack success.

340     **Attack Implementation Details** Our AOH attack aims to induce object hallucination with visu-  
 341     ally subtle perturbations. We compare our method against several baselines:  
 342

- 343     • **Clean (None):** The original, unperturbed video. This serves as the baseline for ideal model  
 344     performance, where Vid-LLMs are expected to correctly identify the absence of the target object.
- 345     • **Random Noise (Random):** Adversarial videos are generated by adding random Gaussian noise  
 346     to the clean video. The noise is scaled such that its maximum perturbation matches our  $\ell_\infty$  budget,  
 347     i.e., with a standard deviation derived from  $\epsilon^2$ , mirroring settings in prior (Li et al., 2024). This  
 348     baseline assesses whether generic noise can induce hallucination.
- 349     • **Random Noise with Mask Assistance (Random&Mask):** Similar to the Random Noise base-  
 350     line, but noise is applied only within the spatial and temporal regions defined by the target object’s  
 351     mask. This explores whether localizing random perturbations to the target area enhances halluci-  
 352     nation.
- 353     • **Our Attack (AOH):** We implement AOH using Projected Gradient Descent (PGD) to optimize the  
 354     intermediate feature alignment objective. We perform 300 optimization steps. The perturbation  
 355     budget is set to  $\epsilon = 8$  under an  $\ell_\infty$  constraint, i.e.,  $\|x_{cle} - x_{adv}\|_\infty \leq 8$ . This is a widely adopted  
 356     setting in adversarial literature (Madry et al., 2018; Zhao et al., 2023) to ensure that adversarial  
 357     perturbations remain visually subtle, given that pixel values are normalized to [0, 255].

358     **Dataset Usage** For all experiments, we employ our carefully curated multi-source benchmark  
 359     dataset, which contains 535 clean/target video pairs. Each clean video  $x_{cle}$  and its corresponding  
 360     target video  $x_{tar}$  is annotated with VQA pairs (e.g., “Is there a car passing the intersection?”) and  
 361     their ground-truth answers: CA (the correct answer when the queried object is absent) and TA (the  
 362     correct answer when the queried object is present). In the evaluation, when the queried object is  
 363     absent, models are expected to generate answers consistent with CA. Conversely, when the queried  
 364     object is supposed to appear, a hallucination is considered successful if the model’s response matches  
 365     TA, indicating that it perceives the non-existent object.

## 367     5.2 ATTACK PERFORMANCE

368     We evaluate the overall effectiveness of our proposed AOH attack against various Vid-LLMs, com-  
 369     paring it with baseline attack methods (Random Noise, Random Noise with Mask Assistance)  
 370     and the model’s performance on clean videos (None baseline). Table 1 summarizes the Acc and  
 371     ChatGPT-3.5 Score across all tested models.

372     Across all evaluated Vid-LLMs, our AOH attack consistently achieves significantly higher object  
 373     hallucination rates (Acc) and more semantically rich hallucinated descriptions (Score) compared to  
 374     all baselines. The “None” baseline, representing the model’s false positive rate on clean videos,  
 375     shows relatively low Acc (ranging from 0.141 to 0.348) and Score (from 1.153 to 2.148). Random  
 376     noise baselines (“Rand.” and “Rand.&Mask”) offer only marginal improvements over “None”, indi-  
 377     cating that generic or localized random perturbations are largely ineffective for inducing targeted se-

378  
 379 Table 1: Main experimental results of AOH attack on various Vid-LLMs. “Clean” and “Target”  
 380 represent the model’s baseline performance on unperturbed clean and target videos, respectively.  
 381 “None”, “Random”, “Random&Mask”, and “Ours” denote the performance under no attack, random  
 382 noise, masked random noise, and our AOH attack. Higher Acc and Score under “Ours” indicate  
 383 greater attack success. “Evaluation” assesses the model’s basic capability: “Clean” uses  $x_{cle}$  as  
 384 input with CA as the answer, while “Target” uses  $x_{tar}$  as input with TA as the answer.

385 Vid model	386 Metric	387 Evaluation		388 Attacking method			389 Other info.	
		390 Clean	391 Target	392 None	393 Rand.	394 R.&M.	395 Ours	396 # Param.
397 LLaVA-Onevision 0.5B	398 Acc	399 0.449	400 0.593	401 0.157	402 0.159	403 0.200	404 <b>0.607</b>	405 894M
	Score	1.863	3.198	1.279	1.319	1.514	<b>3.258</b>	
406 InternVL2.5 1B	407 Acc	408 0.350	409 0.580	410 0.209	411 0.218	412 0.223	<b>0.413</b>	413 938M
	Score	1.659	3.236	1.477	1.490	1.526	<b>2.438</b>	
414 VideoLLaMA3 2B	415 Acc	416 0.480	417 0.142	418 0.141	419 0.146	420 0.164	<b>0.495</b>	421 1.96B
	Score	1.986	1.173	1.153	1.182	1.220	<b>2.695</b>	
422 InternVL2.5 2B	423 Acc	424 0.461	425 0.614	426 0.187	427 0.204	428 0.211	<b>0.506</b>	429 2.21B
	Score	1.881	3.321	1.389	1.423	1.503	<b>2.820</b>	
430 InternVL2.5 4B	431 Acc	432 0.384	433 0.631	434 0.245	435 0.245	436 0.263	<b>0.395</b>	437 3.71B
	Score	1.692	3.411	1.596	1.618	1.681	<b>2.277</b>	
438 Video-ChatGPT 7B	439 Acc	440 0.123	441 0.582	442 0.348	443 0.346	444 0.362	<b>0.402</b>	445 ~8B
	Score	0.838	3.169	2.148	2.117	2.180	<b>2.348</b>	
446 LLaVA-Onevision 7B	447 Acc	448 0.434	449 0.596	450 0.142	451 0.153	452 0.227	<b>0.386</b>	453 8.03B
	Score	1.850	3.249	1.314	1.319	1.611	<b>2.359</b>	
454 VideoLLaMA3 7B	455 Acc	456 0.438	457 0.166	458 0.168	459 0.175	460 0.180	<b>0.586</b>	461 8.04B
	Score	1.906	1.323	1.337	1.323	1.377	<b>3.209</b>	
462 InternVL2.5 8B	463 Acc	464 0.381	465 0.640	466 0.227	467 0.214	468 0.240	<b>0.465</b>	469 8.08B
	Score	1.692	3.423	1.553	1.559	1.634	<b>2.609</b>	

406  
 407 mantic hallucinations. In stark contrast, AOH significantly boosts Acc (e.g., LLaVA-OneVison 0.5B  
 408 from 0.157 to 0.607, VideoLLaMA3 7B from 0.168 to 0.586) and Score (e.g., LLaVA-OneVison  
 409 0.5B from 1.279 to 3.258, VideoLLaMA3 7B from 1.337 to 3.209), demonstrating its superior ca-  
 410 pability in implanting specific object semantics.

411 Notably, for models like LLaVA-OneVison 0.5B, AOH’s Acc (0.607) even surpasses the model’s  
 412 performance on the actual target videos (Target Acc: 0.593), suggesting that AOH can make the  
 413 model perceive non-existent objects more reliably than it detects truly present ones. Similarly, for  
 414 VideoLLaMA3 7B, AOH’s Score (3.209) is exceptionally close to the model’s Score on target videos  
 415 (3.249 from InternVL2.5 8B), showcasing the high fidelity of the hallucinated object’s description.  
 416 VideoLLaMA3 2B and 7B exhibit surprisingly low “Target” Acc and Score, indicating a struggle  
 417 to accurately identify or describe the object even when explicitly present. However, AOH still dra-  
 418 matically increases their Acc and Score, forcing them to hallucinate effectively, which underscores  
 419 AOH’s ability to manipulate underlying feature representations regardless of the model’s inherent  
 420 detection robustness.

### 421 5.3 EXPERIMENTAL ANALYSIS

423 **Cross-Scale Transferability** A critical finding of our study is the alarming cross-model transfer-  
 424 ability of AOH adversarial examples. We investigate this phenomenon by generating adversarial  
 425 videos using LLaVA-OneVison-0.5B and LLaVA-OneVison-7B, and then evaluating their perfor-  
 426 mance when applied to the other model. Results are presented in Table 2. The most striking ob-  
 427 servation is the transferability from the smaller LLaVA-OneVison-0.5B to its larger counterpart,  
 428 LLaVA-OneVison-7B. Adversarial samples crafted for the 0.5B model achieve an Acc of 0.533 and  
 429 a Score of 3.018 when attacking the 7B model. This performance is remarkably higher than the  
 430 7B model’s own-generated adversarial samples (Acc 0.386, Score 2.359). This surprising result  
 431 highlights a dangerous possibility: attackers can design adversarial samples against smaller, com-  
 432 putationally less expensive models, and these samples not only transfer to larger, more complex

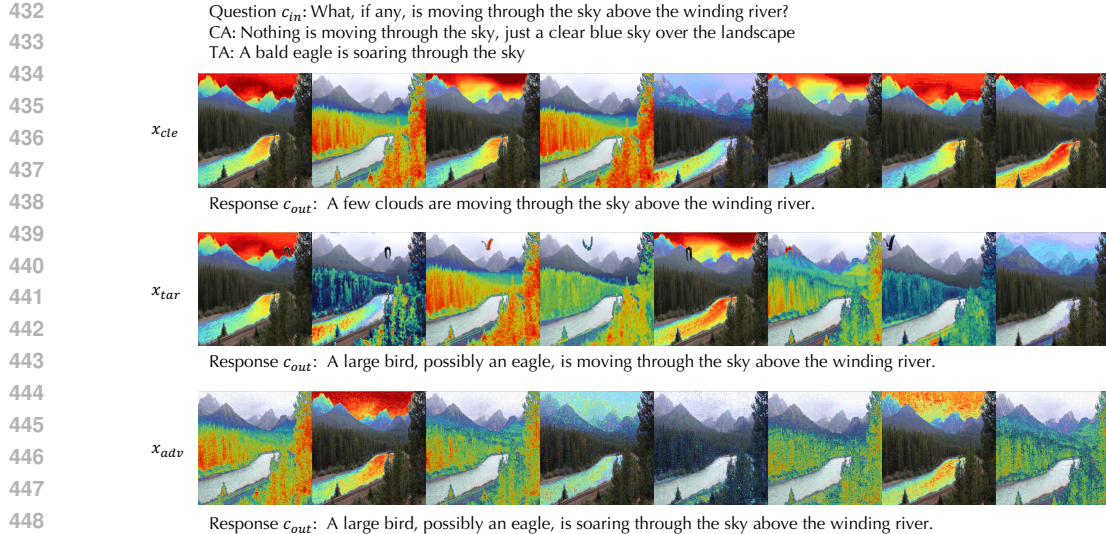


Figure 2: GradCAM visualizations on a clean video (top), its target video (middle), and AOH adversarial counterpart (bottom).

systems but often achieve superior attack efficacy at a fraction of the cost. Conversely, adversarial samples generated for the 7B model show reduced, though still present, attack performance when transferred to the 0.5B model (Acc 0.312, Score 1.998), suggesting an asymmetric transferability where attacks from smaller to larger models are particularly potent. This discovery exposes a profound and cost-effective vulnerability in Vid-LLMs, demanding urgent attention.

**GradCAM for Attack Mechanism Explanation** To shed light on how Vid-LLMs process AOH-perturbed videos, we extend the traditional GradCAM technique to video-text tasks, providing visual explanations of model attention. Using LLaVA-OneVison-7B as an example, our GradCAM visualizations reveal that even when the model successfully hallucinates an object, its attention is not unnaturally focused on the regions where the target object is supposedly introduced. Instead, the model’s attention predominantly remains on naturally existing objects and salient areas within the video. This indicates that our AOH attack is highly covert; it manipulates the model’s internal representations without forcing an overt shift in its visual attention towards the hallucinated entity, making the attack difficult to detect through traditional interpretability methods. Visual examples of GradCAM on clean and adversarial videos are presented in Figure 2.

## 6 CONCLUSION

In this paper, we introduced Adversarial Object Hallucination (AOH), a novel white-box attack revealing semantic vulnerabilities in Video Large Language Models (Vid-LLMs). Through intermediate feature alignment, AOH effectively induces targeted object hallucinations with visually subtle perturbations, significantly outperforming baselines. Critically, we uncovered an alarming **cross-scale transferability** where adversarial examples crafted for smaller models achieve superior efficacy on larger Vid-LLMs of the same architecture, presenting a potent and cost-effective threat. Our analysis further confirmed AOH’s covert nature, manipulating models via semantically structured perturbations without obvious shifts in visual attention. This work highlights a severe vulnerability in Vid-LLMs, underscoring the urgent need for robust internal representations and providing a foundational framework for future adversarial research in multimodal AI safety.

Table 2: Cross-model transferability results for AOH attacks between LLaVA-OneVison 0.5B (LLaVA-OV 0.5B) and 7B models (LLaVA-OV 7B). “Before” refers to the attack performance on the original target model (e.g., 0.5B generated for 0.5B). “After” refers to the attack performance when transferred to the other model (e.g., 0.5B generated then tested on 7B).

Vid model	Before		After	
	Acc	Score	Acc	Score
LLaVA-OV 0.5B	<b>0.607</b>	<b>3.258</b>	0.312	1.998
LLaVA-OV 7B	0.386	2.359	<b>0.533</b>	<b>3.018</b>

486 REFERENCES  
487

488 Tom B. Brown, Benjamin Mann, Nick Ryder, Melanie Subbiah, Jared Kaplan, Prafulla Dhari-  
489 wal, Arvind Neelakantan, Pranav Shyam, Girish Sastry, Amanda Askell, Sandhini Agarwal,  
490 Ariel Herbert-Voss, Gretchen Krueger, Tom Henighan, Rewon Child, Aditya Ramesh, Daniel M.  
491 Ziegler, Jeffrey Wu, Clemens Winter, Christopher Hesse, Mark Chen, Eric Sigler, Mateusz Litwin,  
492 Scott Gray, Benjamin Chess, Jack Clark, Christopher Berner, Sam McCandlish, Alec Radford,  
493 Ilya Sutskever, and Dario Amodei. Language models are few-shot learners. In *Advances in Neu-  
494 ral Information Processing Systems 33: Annual Conference on Neural Information Processing  
495 Systems 2020, NeurIPS 2020, December 6-12, 2020, virtual*, 2020.

496 Nicholas Carlini, Anish Athalye, Nicolas Papernot, Wieland Brendel, Jonas Rauber, Dimitris  
497 Tsipras, Ian J. Goodfellow, Aleksander Madry, and Alexey Kurakin. On evaluating adversarial  
498 robustness. *CoRR*, abs/1902.06705, 2019.

499 Zhe Chen, Jiannan Wu, Wenhui Wang, Weijie Su, Guo Chen, Sen Xing, Muyan Zhong, Qinglong  
500 Zhang, Xizhou Zhu, Lewei Lu, Bin Li, Ping Luo, Tong Lu, Yu Qiao, and Jifeng Dai. Internvl:  
501 Scaling up vision foundation models and aligning for generic visual-linguistic tasks. *CoRR*,  
502 abs/2312.14238, 2023.

503 Zesen Cheng, Sicong Leng, Hang Zhang, Yifei Xin, Xin Li, Guanzheng Chen, Yongxin Zhu, Wenqi  
504 Zhang, Ziyang Luo, Deli Zhao, and Lidong Bing. Videollama 2: Advancing spatial-temporal  
505 modeling and audio understanding in video-llms. *CoRR*, abs/2406.07476, 2024.

506 Suhwan Cho, Seoung Wug Oh, Sangyoun Lee, and Joon-Young Lee. Elevating flow-guided video  
507 inpainting with reference generation. In *AAAI-25, Sponsored by the Association for the Advance-  
508 ment of Artificial Intelligence, February 25 - March 4, 2025, Philadelphia, PA, USA*, pp. 2527–  
509 2535. AAAI Press, 2025.

510 Ian J. Goodfellow, Jonathon Shlens, and Christian Szegedy. Explaining and harnessing adversarial  
511 examples. In *3rd International Conference on Learning Representations, ICLR 2015, San Diego,  
512 CA, USA, May 7-9, 2015, Conference Track Proceedings*, 2015.

513 Kai Hu, Weichen Yu, Li Zhang, Alexander Robey, Andy Zou, Chengming Xu, Haoqi Hu, and  
514 Matt Fredrikson. Transferable adversarial attacks on black-box vision-language models. *CoRR*,  
515 abs/2505.01050, 2025.

516 Linhao Huang, Xue Jiang, Zhiqiang Wang, Wentao Mo, Xi Xiao, Bo Han, Yongjie Yin, and Feng  
517 Zheng. Image-based multimodal models as intruders: Transferable multimodal attacks on video-  
518 based mllms. *CoRR*, abs/2501.01042, 2025.

519 Haibo Jin, Leyang Hu, Xinuo Li, Peiyan Zhang, Chonghan Chen, Jun Zhuang, and Haohan  
520 Wang. Jailbreakzoo: Survey, landscapes, and horizons in jailbreaking large language and vision-  
521 language models. *CoRR*, abs/2407.01599, 2024.

522 Bo Li, Yuanhan Zhang, Dong Guo, Renrui Zhang, Feng Li, Hao Zhang, Kaichen Zhang, Peiyuan  
523 Zhang, Yanwei Li, Ziwei Liu, and Chunyuan Li. Llava-onevision: Easy visual task transfer.  
524 *Trans. Mach. Learn. Res.*, 2025, 2025.

525 Jinmin Li, Kuofeng Gao, Yang Bai, Jingyun Zhang, Shutao Xia, and Yisen Wang. Fmm-attack: A  
526 flow-based multi-modal adversarial attack on video-based llms. *CoRR*, abs/2403.13507, 2024.

527 Shanchuan Lin, Andrey Ryabtsev, Soumyadip Sengupta, Brian L. Curless, Steven M. Seitz, and Ira  
528 Kemelmacher-Shlizerman. Real-time high-resolution background matting. In *IEEE Conference  
529 on Computer Vision and Pattern Recognition, CVPR 2021, virtual, June 19-25, 2021*, pp. 8762–  
530 8771. Computer Vision Foundation / IEEE, 2021.

531 Haotian Liu, Chunyuan Li, Qingyang Wu, and Yong Jae Lee. Visual instruction tuning. In *Ad-  
532 vances in Neural Information Processing Systems 36: Annual Conference on Neural Information  
533 Processing Systems 2023, NeurIPS 2023, New Orleans, LA, USA, December 10 - 16, 2023*, 2023.

540 Muhammad Maaz, Hanoona Abdul Rasheed, Salman Khan, and Fahad Khan. Video-chatgpt: To-  
 541 wards detailed video understanding via large vision and language models. In *Proceedings of the*  
 542 *62nd Annual Meeting of the Association for Computational Linguistics (Volume 1: Long Papers)*,  
 543 *ACL 2024, Bangkok, Thailand, August 11-16, 2024*, pp. 12585–12602. Association for Computa-  
 544 tional Linguistics, 2024.

545 Haley MacLeod, Cynthia L. Bennett, Meredith Ringel Morris, and Edward Cutrell. Understanding  
 546 blind people’s experiences with computer-generated captions of social media images. In *Proceed-  
 547 ings of the 2017 CHI Conference on Human Factors in Computing Systems, Denver, CO, USA,*  
 548 *May 06-11, 2017*, pp. 5988–5999. ACM, 2017.

549 Aleksander Madry, Aleksandar Makelov, Ludwig Schmidt, Dimitris Tsipras, and Adrian Vladu. To-  
 550 wards deep learning models resistant to adversarial attacks. In *6th International Conference on*  
 551 *Learning Representations, ICLR 2018, Vancouver, BC, Canada, April 30 - May 3, 2018, Confer-  
 552 ence Track Proceedings*. OpenReview.net, 2018.

553 Trisha Mittal, Ritwik Sinha, Viswanathan Swaminathan, John P. Collomosse, and Dinesh Manocha.  
 554 Video manipulations beyond faces: A dataset with human-machine analysis. In *IEEE/CVF Winter*  
 555 *Conference on Applications of Computer Vision Workshops, WACV 2023 - Workshops, Waikoloa,*  
 556 *HI, USA, January 3-7, 2023*, pp. 643–652. IEEE, 2023.

557 Nikhila Ravi, Valentin Gabeur, Yuan-Ting Hu, Ronghang Hu, Chaitanya Ryali, Tengyu Ma, Haitham  
 558 Khedr, Roman Rädle, Chloé Rolland, Laura Gustafson, Eric Mintun, Junting Pan, Kalyan Va-  
 559 sudev Alwala, Nicolas Carion, Chao-Yuan Wu, Ross B. Girshick, Piotr Dollár, and Christoph  
 560 Feichtenhofer. SAM 2: Segment anything in images and videos. In *The Thirteenth International*  
 561 *Conference on Learning Representations, ICLR 2025, Singapore, April 24-28, 2025*. OpenRe-  
 562 view.net, 2025.

563 Hugo Touvron, Thibaut Lavril, Gautier Izacard, Xavier Martinet, Marie-Anne Lachaux, Timothée  
 564 Lacroix, Baptiste Rozière, Naman Goyal, Eric Hambro, Faisal Azhar, Aurélien Rodriguez, Ar-  
 565 mand Joulin, Edouard Grave, and Guillaume Lample. Llama: Open and efficient foundation  
 566 language models. *CoRR*, abs/2302.13971, 2023.

567 Yubo Wang, Chaohu Liu, Yanqiu Qu, Haoyu Cao, Deqiang Jiang, and Linli Xu. Break the visual  
 568 perception: Adversarial attacks targeting encoded visual tokens of large vision-language models.  
 569 In *Proceedings of the 32nd ACM International Conference on Multimedia, MM 2024, Melbourne,*  
 570 *VIC, Australia, 28 October 2024 - 1 November 2024*, pp. 1072–1081. ACM, 2024.

571 Jianzong Wu, Xiangtai Li, Chenyang Si, Shangchen Zhou, Jingkang Yang, Jiangning Zhang, Yining  
 572 Li, Kai Chen, Yunhai Tong, Ziwei Liu, and Chen Change Loy. Towards language-driven video  
 573 inpainting via multimodal large language models. In *IEEE/CVF Conference on Computer Vision*  
 574 *and Pattern Recognition, CVPR 2024, Seattle, WA, USA, June 16-22, 2024*, pp. 12501–12511.  
 575 IEEE, 2024.

576 Sibo Yi, Yule Liu, Zhen Sun, Tianshuo Cong, Xinlei He, Jiaxing Song, Ke Xu, and Qi Li. Jailbreak  
 577 attacks and defenses against large language models: A survey. *CoRR*, abs/2407.04295, 2024.

578 Fisher Yu, Haofeng Chen, Xin Wang, Wenqi Xian, Yingying Chen, Fangchen Liu, Vashisht Mad-  
 579 havan, and Trevor Darrell. BDD100K: A diverse driving dataset for heterogeneous multitask  
 580 learning. In *2020 IEEE/CVF Conference on Computer Vision and Pattern Recognition, CVPR*  
 581 *2020, Seattle, WA, USA, June 13-19, 2020*, pp. 2633–2642. Computer Vision Foundation / IEEE,  
 582 2020.

583 Boqiang Zhang, Kehan Li, Zesen Cheng, Zhiqiang Hu, Yuqian Yuan, Guanzheng Chen, Sicong  
 584 Leng, Yuming Jiang, Hang Zhang, Xin Li, Peng Jin, Wenqi Zhang, Fan Wang, Lidong Bing, and  
 585 Deli Zhao. Videollama 3: Frontier multimodal foundation models for image and video under-  
 586 standing. *CoRR*, abs/2501.13106, 2025a.

587 Hang Zhang, Xin Li, and Lidong Bing. Video-llama: An instruction-tuned audio-visual language  
 588 model for video understanding. In Yansong Feng and Els Lefever (eds.), *Proceedings of the*  
 589 *2023 Conference on Empirical Methods in Natural Language Processing, EMNLP 2023 - System*  
 590 *Demonstrations, Singapore, December 6-10, 2023*, pp. 543–553. Association for Computational  
 591 Linguistics, 2023.

594 Jiaming Zhang, Junhong Ye, Xingjun Ma, Yige Li, Yunfan Yang, Yunhao Chen, Jitao Sang, and  
595 Dit-Yan Yeung. Anyattack: Towards large-scale self-supervised adversarial attacks on vision-  
596 language models. In *IEEE/CVF Conference on Computer Vision and Pattern Recognition, CVPR*  
597 *2025, Nashville, TN, USA, June 11-15, 2025*, pp. 19900–19909. Computer Vision Foundation /  
598 IEEE, 2025b.

599 Yunqing Zhao, Tianyu Pang, Chao Du, Xiao Yang, Chongxuan Li, Ngai-Man Cheung, and Min Lin.  
600 On evaluating adversarial robustness of large vision-language models. In *Advances in Neural In-*  
601 *formation Processing Systems 36: Annual Conference on Neural Information Processing Systems*  
602 *2023, NeurIPS 2023, New Orleans, LA, USA, December 10 - 16, 2023*, 2023.

603 Wanqi Zhou, Shuanghao Bai, Qibin Zhao, and Badong Chen. Revisiting the adversarial robustness  
604 of vision language models: a multimodal perspective. *CoRR*, abs/2404.19287, 2024.

605 Deyao Zhu, Jun Chen, Xiaoqian Shen, Xiang Li, and Mohamed Elhoseiny. Minigpt-4: Enhancing  
606 vision-language understanding with advanced large language models. In *The Twelfth Interna-*  
607 *tional Conference on Learning Representations, ICLR 2024, Vienna, Austria, May 7-11, 2024*.  
608 OpenReview.net, 2024. URL <https://openreview.net/forum?id=1tZbq88f27>.

609 Andy Zou, Zifan Wang, J. Zico Kolter, and Matt Fredrikson. Universal and transferable adversarial  
610 attacks on aligned language models. *CoRR*, abs/2307.15043, 2023.

611  
612  
613  
614  
615  
616  
617  
618  
619  
620  
621  
622  
623  
624  
625  
626  
627  
628  
629  
630  
631  
632  
633  
634  
635  
636  
637  
638  
639  
640  
641  
642  
643  
644  
645  
646  
647